PERGAMON

International Journal of Heat and Mass Transfer 44 (2001) 4557–4561

International Journal of HEAT and MASS TRANSFER

www.elsevier.com/locate/ijhmt

Technical Note

Prediction of CHF enhancement due to flow obstacles

Y. Guo [a,*], D.C. Groeneveld [a,b], S.C. Cheng [a]

[a] Department of Mechanical Engineering, University of Ottawa, 770 King Edward Avenue, P.O. Box 450, Stn. A, Ottawa, ON, Canada, K1N 6N5

[b] Fuel Channel Thermalhydraulics Branch, Chalk River Laboratories, Atomic Energy of Canada Limited, Chalk River, ON, Canada, K0J 1J0

Received 4 October 2000; received in revised form 22 February 2001

Abstract

A semi-theoretical prediction method of CHF enhancement due to flow obstacles inserted in a flow channel was developed in this paper. Compared to the existing CHF enhancement equations, the present prediction model includes the effect of most of the important parameters and correctly represents the observed parametric and asymptotic trends. Good agreement has been found between the model predictions and the existing experimental databases. © 2001 Elsevier Science Ltd. All rights reserved.

Keywords: Critical heat flux; CHF; Enhancement; Obstacle; Prediction model

1. Introduction

There is ample experimental evidence that flow obstructions can significantly enhance the critical heat flux (CHF) [1–3]. Several simplistic methods have been proposed; however none of them adequately represent the observed trends. This technical note presents a semi-analytical method, which can simultaneously predict the observed parametric trends of flow, quality, obstacle-shape, flow blockage ratio and distance downstream from the obstacle.

2. CHF mechanisms

At low flow qualities, the flow regime is either bubbly flow or annular flow with a thick liquid film on the wall. Here the CHF occurs because of an inadequate removal of bubbles from the wall (DNB-type crisis) and/or a depletion of the liquid film on the wall (entrainment-controlled film-dryout). The CHF vs x curve in this region is smooth; hence there is a gradual change in CHF mechanism between DNB and entrainment-controlled dryout. At higher flow qualities, the flow regime is also annular flow but the liquid film is very thin and the primary supply of liquid in the film is by deposition from the entrained droplets in the core region ("deposition-controlled dryout"). The changeover to deposition-controlled dryout takes place in the limiting quality region where the CHF drops sharply compared to the smooth decline in CHF with critical quality (the quality at CHF location) elsewhere.

Because of this difference in CHF mechanisms, the physics of CHF enhancement due to the presence of obstacles must also be different for these two quality regions. Different prediction methods for CHF enhancement are therefore developed for each quality region.

3. CHF enhancement in the lower quality region

The lower quality region includes both the bubbly flow regime and the "entrainment-controlled" annular flow regime. Here the insertion of flow obstacles in a flow channel enhances the CHF by (a) an increase of flow turbulence, which both increases the wall–liquid heat

* Corresponding author. Tel.: +1-613-562-5800; fax: +1-613-562-5177.

E-mail address: yguo@uottawa.ca (Y. Guo).

PII: S0017-9310(01)00088-6

Nomenclature

CHF	critical heat flux, kw/m^2
CHF_0	critical heat flux without obstacles, kw/m^2
D	inside diameter, m
f_{eff}	effective friction coefficient
$G = \rho u$	mass flux, $kg/m^2 s$
h_{fg}	latent heat of vaporization, J/kg
k_ε	local resistance coefficient caused by obstacles
k_s	coefficient standing for shape and location effects of obstacles
k_D	deposition rate, m/s
L_{SP}	grid spacing, m
R_{CHF}	relative CHF enhancement
Re	Reynolds number
x	vapor quality
x_0	vapor quality at the location of the obstacle
x_{lim}	limiting critical quality
We	Weber number
Greek symbols	
β	obstacle-edge-coefficient modifying local resistance
ε	blockage ratio (flow obstruction cross-section area/channel flow area) (%)
μ	viscosity, kg/m s
ρ	density, kg/m^3
σ	surface tension, N/m
Subscripts	
D	deposition-controlled region
E	entrainment-controlled region
f	liquid (referred to fluid at saturation temperature)
g	vapor (referred to vapor at saturation temperature)

transfer and facilitates the bubble detachment, and (b) a change of phase distribution. These two effects on CHF can both be expressed by the generally accepted exponential decaying function [9,12]:

$$R_{CHF,E} = CHF/CHF_0 - 1 = b e^{-aL_{SP}/D}, \quad (1)$$

where R_{CHF} is the relative CHF enhancement. Once turbulence is induced by an obstacle, it will travel downstream and the intensity of the turbulence will decay. The decay function depends on how far the turbulence can reach and how fast the turbulence weakens. According to experimental observations and the relaxation theory [4], a increases with a decrease in the liquid velocity u_f and an increase in the liquid viscosity μ_f. Assuming zero slip, these trends can be represented by

$$a = a_1 Re_{f0}^{-a_2} = a_1 \{GD/\mu_f[(1 - x_0) + \rho_g/\rho_f x_0]\}^{-a_2}, \quad (2)$$

where Re_{f0} refers to the liquid Reynolds number at the obstacle location. Based on the experimental data [6], optimized values for a_1 and a_2 are 2.45 and 0.311, respectively.

The coefficient 'b' in Eq. (1), which is the amplitude of CHF enhancement, is affected by (i) the increased turbulence level, which increases the heat and momentum transfer, and (ii) the effect of phase redistribution caused by obstacles. The heat transfer enhancement can be analyzed in single-phase flow by the well-known Reynolds analogy between heat and momentum transfer, $St = f_{eff}/2$, in which the Stanton number is defined as $St = h_c/(\rho_f u_f C_{pf})$. f_{eff} denotes the effective friction coefficient, which represents either the friction coefficient (f) in bare tubes or the sum of the friction coefficient and the local resistance coefficient (k_ε) in tubes with obstacles. From this theory one can represent the relative increase in single-phase heat transfer due to the obstacle as

$$b_{h,t} = (h_{c,ob} - h_c)/h_c = b_h k_\varepsilon \beta/f, \quad (3)$$

where β is the obstacle-edge-coefficient suggested by Groeneveld [2], varies from 1.0 for obstacles with abrupt leading edge to 0.3 for obstacles with streamlined shape. If we assume that the relative CHF enhancement is proportional to the relative enhancement in single-phase heat transfer, then

$$b_{CHF,t} = b_1 k_\varepsilon \beta/f \quad (4)$$

in which, b_1 will be determined by experimental data.

The change of phase distribution is more complex. It strongly depends on the shape, edge and location of the obstacle [5]. Usually, an obstacle with a blunt (90°) leading edge tends to give a random disturbance; hence it makes the phase distribution more uniform. However, an obstacle with pointed leading edge or a streamlined obstacle may deflect the flow or one of the phases, rather than providing a random disturbance. A ring type obstacle tends to strip the liquid off the wall, or confines the liquid phase to the core region and leaves more vapor near the wall. Such effects are negative and decrease the CHF in the entrainment-controlled region. These effects can be qualitatively analyzed to be proportional to the relative height of obstacles in radius direction, which can be represented by the proportionality to the flow blockage ratio. With an increase in quality and Reynolds number, these effects gradually disappear because the very high disturbance results in a more homogeneous flow. Therefore, one can approximately express the negative effects by

$$b_{\mathrm{CHF,r}} = k_s b_2 \varepsilon (1 - x_0) Re_{m0}^{-n}, \tag{5}$$

where k_s is the coefficient representing the shape and location effects of the obstacles, b_2 and n are empirical constants determined by fitting experimental data, Re_{m0} is the homogeneous Reynolds number and x_0 is the quality at the obstacle location. Obstacles that only obstruct the flow away from the heated surface will not have a negative effect on CHF enhancement and therefore, their k_s value will be zero. Ring type obstacles however result in a detrimental redistribution of the wall liquid and k_s should be unity. Therefore, k_s can be written as the ratio of wetted perimeter contacted by obstacles (P_{oc}) to the total wetted perimeter of the flow channel (P), that is $k_s = P_{oc}/P$.

Finally, the relative CHF enhancement for the pre-limiting quality region can be expressed as

$$R_{\mathrm{CHF,E}} = \left[b_1 \beta k_\varepsilon / f - b_2 \varepsilon P_{oc}/P(1 - x_0) Re_{m0}^{-n}\right] \mathrm{e}^{-aL_{\mathrm{SP}}/D}. \tag{6}$$

By best fitting to experimental data [6], b_1, b_2 and n are determined as 0.0048, 2.0E7 and 1.25, respectively. In Eq. (6), the local drag coefficient k_ε is based on Voj equation [2] but is modified by replacing ε in the numerator with $\sqrt{\varepsilon}$ to improve the agreement with our experimental data.

$$k_\varepsilon = \sqrt{\varepsilon}/(1 - \varepsilon)\left[2.12 + 10^4 (1 - \varepsilon)^2 / Re_{f0}\right]. \tag{7}$$

The fanning friction factor $f = 0.046/Re_{f0}^{0.2}$ is used in Eq. (6).

4. CHF enhancement in the deposition-controlled region

In this region, the flow regime is annular flow with a very thin liquid film ($\ll$1 mm) on the wall (most liquid is entrained in the core region). Here the primary mechanism of CHF enhancement is the increase in turbulence of the droplet-laden gas stream, which results in a significant increase in deposition coefficient. The resulting CHF enhancement decays with distance downstream from the obstacle.

The gradient in liquid-film flow rate can be expressed as:

$$\mathrm{d}W_{\mathrm{lf}}/\mathrm{d}z = (k_D C - E - q/h_{\mathrm{fg}})\pi D, \tag{8}$$

where W_{lf} is the liquid-film flow rate, C is the droplet concentration, k_D is the deposition coefficient, and E is the liquid-film entrainment rate. Since E and $\mathrm{d}W_{\mathrm{lf}}/\mathrm{d}z$ are approximately zero for the thin-film deposition-controlled region, the CHF is proportional to the deposition rate (k_D). Thus the relative CHF enhancement, R_{CHF}, will be proportional to the relative increase of deposition rate ($k_{D\varepsilon}/k_D - 1$) where $k_{D\varepsilon}$ denotes the deposition coefficient with obstacles. R_{CHF} is also assumed to be inversely proportional to the Reynolds number, since at high Re values the higher turbulence level has already a significant higher deposition rate, where a further increase in turbulence level due to obstacles will result in a relatively small increase in R_{CHF}. These effects are all assumed to decay exponentially as shown in the following equation for R_{CHF}:

$$R_{\mathrm{CHF,D}} = c_1' (k_{D\varepsilon} - k_D)/k_D Re_v^{-m} \mathrm{e}^{-c_2 L_{\mathrm{SP}}/D}, \tag{9}$$

where c_1', c_2 and m are experimentally determined constants, $Re_v = GD/\mu_v$. Substituting $k_{D\varepsilon} = (1.4416\varepsilon + 1)k_D$ as suggested by Windecker et al. [7], Eq. (9) can be rewritten as

$$R_{\mathrm{CHF,D}} = c_1 \varepsilon / Re_v^m \mathrm{e}^{-c_2 L_{\mathrm{SP}}/D}, \tag{10}$$

where c_1 ($= 1.4416c_1'$). Based on our experimental data a less sensitivity of the relative CHF enhancement to the blockage ratio is found, and then a modification to Eq. (10) is made as

$$R_{\mathrm{CHF,D}} = c_1 \varepsilon^{0.65} / Re_v^m \mathrm{e}^{-c_2 L_{\mathrm{SP}}/D} \tag{11}$$

in which following optimized coefficients are obtained based on Freon data [6]: $c_1 = 1.9\mathrm{E}5$, $m = 0.67$ and $c_2 = 1.0 \times 10^{-6} Re_{m\mathrm{cr}}^{0.8}$, where $Re_{m\mathrm{cr}}$ is the homogeneous Reynolds number based on critical quality.

5. Comparison with data

The CHF enhancement ratio $\mathrm{CHF}/\mathrm{CHF}_0 (= R + 1)$ can finally be predicted with Eqs. (1), (6) and (11), where R is either $R_{\mathrm{CHF,E}}$ or $R_{\mathrm{CHF,D}}$. In the transition between the entrainment-controlled and the deposition-controlled region the CHF enhancement ratio is calculated by interpolation:

$$R_{\mathrm{CHF}} = \begin{cases} R_{\mathrm{CHF,E}} \\ \quad \text{if } x_{\mathrm{cr}} \leqslant 0.9x_{\mathrm{lim}}, \\ (x_{\mathrm{cr}} - 0.9x_{\mathrm{lim}})/(0.2x_{\mathrm{lim}})(R_{\mathrm{CHF,D}} - R_{\mathrm{CHF,E}}) \\ \quad +R_{\mathrm{CHF,D}} \quad \text{if } 0.9x_{\mathrm{lim}} < x_{\mathrm{cr}} < 1.1x_{\mathrm{lim}}, \\ R_{\mathrm{CHF,D}} \\ \quad \text{if } x_{\mathrm{cr}} \geqslant 1.1x_{\mathrm{lim}}, \end{cases} \tag{12}$$

where $x_{\mathrm{lim}} = \max\{0.3,\ [1.0 - 0.86\exp(-19.0We^{-0.5})]\}$, in which, $We = G^2 D/(\rho_f \sigma)$ [1].

Comparisons of CHF enhancement prediction of Eqs. (6) and (11) have been made with Freon data from University of Ottawa [6], Freon and water data from Chalk River Laboratory [8] as well as existing prediction methods. Parametric ranges of data to be compared are given in Table 1. Figs. 1 and 2 are typical results showing the model to be in good agreement with Freon data from University of Ottawa and Chalk River Laboratories. Further comparisons will be made when additional data become available. The model slightly over-predicts the water CHF-enhancement data.

Table 1
Ranges of the database used in the comparison with the model

Reference	Fluid	Parameter range	Type of blockage	Blockage ratio
[6][a]	HFC134a	$P = 0.96$–2.39 MPa $G = 1000$–3000 kg/m^2 s $x_{cr} = 0$–60%	Cylinder, square bar, ring	12%, 24%, 37%
[8]	HFC134a	$P = 1.66$ MPa $G = 2320$–4630 kg/m^2 s $x_{cr} = 0$–30%	Bar, cylindrical button	21.4%, 14.2%
[8]	Water	$P = 10.0$ MPa $G = 3250$–6500 kg/m^2 s $x_{cr} = 0$–30%	Bar, cylindrical button	21.4%, 14.2%

[a] Data in this reference are used to optimize the coefficients in the prediction model.

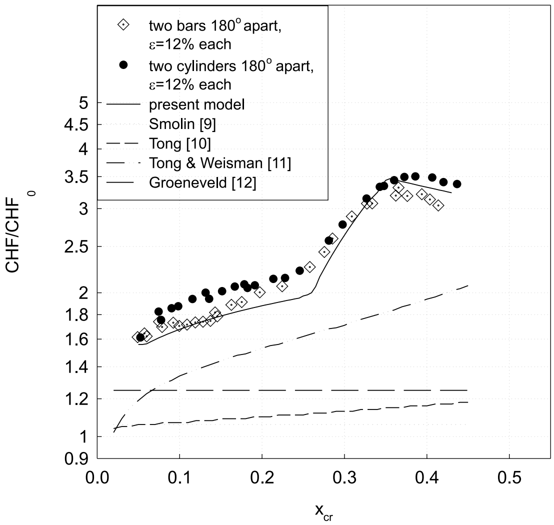

Fig. 1. Comparisons of present model predictions with Freon data from University of Ottawa [6] and existing prediction methods [9–12]: R-134a, $P = 1.67$ MPa, $G = 3000$ kg/m^2 s, $L = 0.45$–2 m, pitch 125 mm.

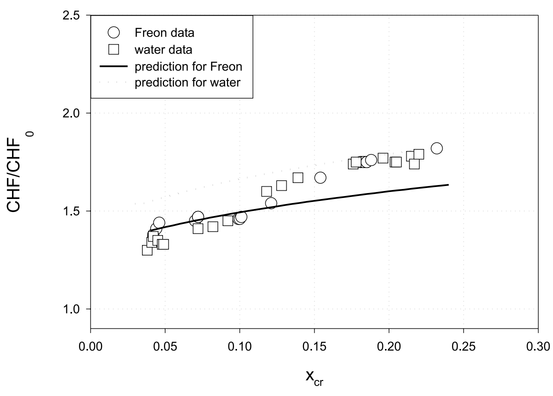

Fig. 2. Comparisons of present model prediction with AECL data: blockage ratio 14.2%, $D = 8$ mm, $G_{water} = 5500$ kg/m^2 s, $P_{water} = 10$ MPa, $G_{Freon} = 3920$ kg/m^2 s, $P_{Freon} = 1.66$ MPa, $L_{SP}/D = 15.625$.

Compared to the existing CHF enhancement equations, the present model includes the effect of most of the important parameters (G, x_{CHF}, ε, L/D, shape and leading/trailing edge) and correctly represents the observed parametric and asymptotic trends. It is thus considered a significant improvement over existing CHF-enhancement prediction methods.

References

[1] I.L. Pioro, S.C. Cheng, A.Z. Vasic, I. Salah, Experimental evaluation of the limiting critical quality values in circular and non-circular flow geometries, Nucl. Eng. Des. 190 (1999) 317–339.

[2] D.C. Groeneveld, W.W. Yousef, Spacing devices for nuclear fuel bundles: a survey of their effect on CHF, post-CHF heat transfer and pressure drop, in: Proceedings of the ANS/ASME Topical Meeting on Nuclear Reactor Thermalhydraulics, Saratoga, New York, October 1980.

[3] S. Doerffer, D.C. Groeneveld, J.R. Schenk, Experimental study of the effects of flow inserts on heat transfer and critical heat flux, in: Proceedings of the Fourth International Conference on Nuclear Engineering, New Orleans, March 10–14, 1996.

[4] M.A. Gotovsky, M.A. Kvetniy, Some problems of Lookup table method usage for CHF determination, in: Proceedings of the Eighth International Conference on Nuclear Engineering, Baltimore, Maryland, April 2–6, 2000.

[5] I.L. Pioro, D.C. Groeneveld, S.C. Cheng, S. Doerffer, A.Z. Vasic, Effect of flow obstruction shape on the critical heat flux, in: Proceedings of the Eighth International Conference on Nuclear Engineering, Baltimore, Maryland, April 2–6, 2000.

[6] I.L. Pioro, S.C. Cheng, A.Z. Vasic, Y. Antoshko, Effects of flow obstructions on the critical heat flux in a vertical circular tube with upward flow of R-134, Internal report of University of Ottawa, UO-MCG-TH-0001, 2000.

[7] U. Windecker, C.Y. Gu, J. Dennhardt, Droplet deposition in the annular flow regime with and without the influence

of a spacer, NURETH-9, San Francisco, California, October 3–8, 1999.
[8] S. Doerffer, Private communication, 2000.
[9] V.N. Smolin, V.K. Polyakov, Coolant boiling crisis in rod assemblies, in: Sixth International Heat Transfer Conference, vol. 5, 1978, pp. 47–52.
[10] L.S. Tong, A phenomenological study of critical heat flux, ASME 75-HT-68, 1975.
[11] L.S. Tong, J. Weisman, Thermal Analysis of Pressurized Water Reactors, third ed., American Nuclear Society, New York, 1996.
[12] D.C. Groeneveld, L.K.H. Leung, J. Zhang, S.C. Cheng, A. Vasic, Effect of appendages on film-boiling heat transfer in tubes, NURETH-9, San Francisco, California, October 3–8, 1999.